CHEMICAL ENGINEERING TRANSACTIONS
VOL. 46, 2015
A publication of AIDIC
The Italian Association of Chemical Engineering
Online at www.aidic.it/cet
Guest Editors: Peiyu Ren, Yancang Li, Huiping Song

ISBN 978-88-95608-37-2; **ISSN** 2283-9216
DOI: 10.3303/CET1546178

Study on the Performances of Two Kinds of Special Tubing Connector

Manlai Zhang[a], Qin Zhang*[a], Li Cheng[b], Ruiquan Liao[b], Jin Feng[a]

[a] School of Mechanical Engineering, Yangtze University, Jingzhou, China
[b] The Branch of Key Laboratory of CNPC for Oil and Gas Production, Yangtze University, Jingzhou, China
caddg@126.com

The connection and sealing performances of two special tubing connectors have been revealed for selection and structure modification, which were designed for use in ultra-deep, sulfur, high pressure wells. This study has used the finite element method to compute the stress and contact pressure of the Premium Shouldered connector under different loads, including the tension, internal pressure and combined load. It showed that the high contact pressure appeared on shoulder and sealing surface / spot once the connector was made up. The shoulder extrusion site and the root of first thread having the maximum Von Mises stress were in plastic state. When the tensile load increased, the stress in the root of first thread at the big end of the tubing enlarged, and the maximum contact pressures on shoulder surfaces decreased form 1172.0 MPa and 1477.0 MPa to 254.9 MPa and 438.9 MPa for PSC-Ⅰ and PSC-Ⅱ respectively. The sealing performance of shoulder degraded and the sealing surface / spot played a major role. Additionally, the worst load conditions affecting the sealing and connection performances were tension load and combined load of "tension + internal pressure" respective, and both kinds of connectors could meet the performance requirements when the loads were 900 kN and 800 KN+40 MPa.

1. Introduction

Safeguarding the down - hole pipe string has been an important task in oil-gas engineering. Compared to the pipe body, the tubing connector is more prone to be destroyed for the reasons of wear, plastic deformation and fracture on the connection of thread, which became the weakest spot of the pipe string (Fransplass et al. (2013); Le et al. (2015); Sønstabø et al. (2015)). Field application approves that the connection and sealing performances of API round threaded decrease significantly when it is exerted with a large axial or radial load in the deep and high-pressure gas well (Baragetti et al. (2009); Ferjani et al. (2011)). So some Premium Shouldered connector (PSC) (Assanell and Dvorkin (1993); Chen et al. (2011)) are designed to conquer the fault with the special sealing style, in which the sealing is not realized through the interference fit of screw threads, but by the contacts between pipe body and coupling at the torque shoulder surface and sealing surfaces, avoiding too large stress on screw threads. However, the connector performances vary significantly with the structures and load (Zanuy et al. (2012); Fransplass et al. (2014); Lorenzini et al. (2015)). For example, one type of premium connection has the fixed connection strength at different bending stress, but the sealing ability decreases sharply for the increasing tensile load (Cui et al. (2015)), which is the same as the long round thread (Yuan et al. (2006)). In order to choose and apply the proper kind of connector for the integrated tubing string, two premium connectors are investigated through the finite element method in this paper.

2. The calculation model

2.1 The connector structure and grid model

Both connectors adopted the trapezoid thread, and the tilt angles of bearing surface and import side were 3° and 10° respectively for PSC-Ⅰ connector, which sealed through two pairs of contacts on shoulders and sealing surfaces (shown in Fig. 1a). Other parameters of PSC-Ⅰ included: Six effective joints, the effective length 19.6 mm, and thread length 63.5 mm.

a PSC-Ⅰ b PSC-Ⅱ

Figure 1: Structures of two Premium Shouldered connectors

For PSC-Ⅱ, the tilt angles of bearing surface and import side were 0° and 45° respectively (Fig. 1b), and two pairs of contacts on spherical surface - cone surface and inner rectangular shoulders were crucial to sealing.
For the convenience of analysis, the small spiral angle of connector was ignored, and construction features of axial symmetry and symmetry about middle cross-section were considered for the building of finite element models. As shown in Fig. 2, the quadrilateral axisymmetric linear reduced integral elements were adopted, in which each node had axial and radial freedoms, but the circumferential displacement was 0. Several assumptions were assumed in numerical calculation: material was isotropic (Yeh et al. (2014)) and isotropic hardenings in post-yield (Aydın et al. (2015)).

a PSC-Ⅰ b PSC-Ⅱ

Figure 2: Mesh models of two Premium Shouldered connectors

2.2 Load condition

After fixing the symmetry plane, the pressure and axial force determined according to the pipe operation condition were respectively exerted on the inner wall and the left side of pipe. When the well depth was 6000 m, the maximum loads of pipe are tension with 900 kN and pressure with 40 MPa. It should be noted that a certain size contact stress was caused on the sealing and shoulder surfaces for the interference fit during make-up, and above loads must be imposed later.
After make-up, the pipe body and connector contact and the moment of annular friction force (M_f) about the central axis balances with the make-up torque (N•m) (Wu et al. (2013)),

$$M_f = \sum \mu F_i r_i = -M_n \tag{1}$$

Where ri is the radius of node about axis, and μ is the friction coefficient with 0.02.
Following Equ.1, the interference fits under different torques were simulated with the sliding coulomb friction model and contact algorithm. The results were shown in Tab. 1.

Table 1: The interference fits with make-up torque

Type	Interference fit on sealing surface (mm)	Interference fit on the shoulder (mm)	Make-up torque (N·m)
PSC-Ⅰ	0.101	0.085	4500
PSC-Ⅱ	0 (Point contact)	0.115	4430

Other related parameters were: tubing size 88.9 mm × 6.45 mm, steel grade G3 125, elastic modulus 200Gpa, Poisson ratio 0.3, and yield strength 860 MPa.

3. Results and discussion

3.1 Make up performance

After make-up, Large Von Mises stress appeared at the zone from shoulder to the first buckle (Fig. 3), and local region around the shoulder was in plastic state without destruction as the stress just exceeded the yield strength slightly. Towards the big end of the tubing, the stress decreased to 0 at the 7th buckle of PSC-Ⅰ and 9th buckle of PSC-Ⅱ.

Figure. 4 shows that the inner wall of tubing before the 6th buckle is compressed, and the maximum compressive stress at the shoulder is 420 MPa for PSC-Ⅰ. Owing to the stress concentration of point-contact sealing in PSC-Ⅱ, the stress increased to 635 MPa.

a PSC-Ⅰ *b. PSC-Ⅱ*

Figure 3: Von Mises stress of connectors after make up

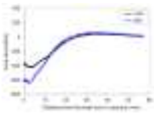

Figure 4: Axial stress of tubing inner wall after make-up

3.2 Effect of axial tensile load

3.2.1 Seal performance

Contact pressure is an important evaluating index of the sealing performance for connector. After make up, interference fit between the pipe body and the joint had larger contact pressure, and the pressure increased at shoulder along the direction of arrow, then decreased rapidly on transition surface, but increased again to a higher value on sealing surface (Fig. 5).

a PSC-Ⅰ *b PSC-Ⅱ*

Figure 5: Contact pressure changes with axial tensile load

When the axial tension increased, the maximum contact pressures on shoulder surfaces individually decreased form 1172.0 MPa and 1477.0 MPa to 254.9 MPa and 438.9 MPa for PSC-Ⅰ and PSC-Ⅱ. Specially, as the tension was larger than 600 kN, the maximal contact pressure on the shoulder surfaces was smaller than on the sealing surface/spot. This indicates the bigger fall range of sealing ability for PSC-Ⅰ, and higher pressure in sealing surface than in the shoulder especial as the force exceeds 600 kN. For PSC-Ⅱ, the maximum contact pressure existed at the contact point is rather steady. Through above analysis, the conclusion that the sealing performances of two connectors mainly depend on the sealing surface / spot can be drawn.

3.2.2 Von Mises Stress distribution

The Von Mises stress was less than the yield strength under different axial loads to meet the strength requirements. As shown in Figs. 6-7, the stress at both ends of thread was larger and the first thread root on the tubing large end gradually entered plastic state with the increasing load, which demonstrated that thread engagement at both ends of the pipe body mainly bore the axial tensile load. Specially, the first thread engagement exerted the most influence over the connection of connector, and other threads could not withstand greater loads anymore once it was destructed.

a Tension 600 KN *b Tension 900 KN*

Figure 6: The Von Mises Stress of PSC-Ⅰ

a Tension 600 KN *b Tension 900 KN*

Figure 7: The Von Mises Stress of PSC-Ⅱ

3.3 Effect of internal pressure

3.3.1 Seal performance

As the tubing acted by internal pressure bulged to extrude the connector, the maximum contact pressure at the reversed oblique shoulder, the sealing surface and the transition surface increased significantly for PSC-Ⅰ, while PSC-Ⅱ changed more slightly (Fig. 8).

a PSC-Ⅰ *b PSC-Ⅱ*

Figure 8: Contact pressure changes with the internal pressure

3.3.2 Von Mises Stress distribution

Figures. 9-10 shows the stress transfer is conducted through the thread engagement between pipe body and connector. With the increase of internal pressure, the stress of pipe body and joint enlarged apparently, but the maximum stress around the small end of pipe body changed minimally.

a Internal pressure 40 MPa *b Internal pressure 70 MPa*

Figure 9: The Von Mises stress of PSC-Ⅰ

a Internal pressure 40 MPa *b Internal pressure 70 MPa*

Figure 10: The Von Mises stress of PSC-Ⅱ

3.4 Effect of combined load

3.4.1 Seal performance

Under combined load "800 KN + different internal pressure", the change rule of contact pressure with the internal pressure was similar with that of single load "internal pressure", but the value of contact pressure was decreased for the tensile load, and the peak point on sealing surface was below than at the shoulder, which indicates the sealing surface plays a key important role on the sealing performance for stretched connector.

a PSC-Ⅰ *b PSC-Ⅱ*

Figure 11: Contact pressure changes with combined load

3.4.2 Von Mises Stress distribution

The maximum Von Mises stress concentrates on both ends of thread and the stress of pipe body raised with the increase of internal pressure, which was more like that of "internal pressure" (shown in Figs. 12-13).

a PSC-Ⅰ *b. PSC-Ⅱ*

Figure 12: Von Mises Stress under the combined load (800 KN+10 MPa)

a PSC-Ⅰ *b. PSC-Ⅱ*

Figure 13: Axial stress of tubing inner wall under different combined loads

4. Conclusions

In summary, we have analyzed the connection and sealing of two PSC under different loads for the connector application. After make-up, two pairs of contact and interference fit at shoulder and sealing surface implement the connector sealing performance. Small plastic deformation happens at the squeezes at the shoulder joint and thread root of the first buckle for the local Von Mises stress exceeding the material yield strength.

The axial tensile load is born by the thread engagement and mainly influenced the stress of the first thread roots on the tubing large end. Therefore, it is advised to improve the connection strength of buckle for enhancing the carrying capacity of connector. With the increase of tension, connector sealing ability declines, which is characterized with the decrease of maximum contact pressure, and PSC-Ⅰ is worse than the PSC-Ⅱ. Specially, contact pressure in sealing surface is higher than in the shoulder as the tension exceeds 600 kN, indicating that the sealing surface / spot played a major role for connector seal. Compared with load conditions of "axial tensile load" and "internal pressure", connection performance degrades most serially under the combined load, and both connectors can meet the performance requirement with the maximum tensile load of 900 KN and “800 KN+40 MPa” respectively.

Acknowledgments

This study was supported by the Natural Science Foundation of Hubei (2015CFC858) and the Doctoral Fund of Education Ministry (20114220110001).

References

Assanell A.P., Dvorkin E.N., 1993, Finite element methods of OCTG threaded connection. Computer & Structures, 47(4-5): 725-734, 10.1016/0045-7949(93)90354-G.

Aydın A.C., Kılıç M., Maali M., Sağıroğlu M., 2015, Experimental assessment of the semi-rigid connections behavior with angles and stiffeners. Journal of Constructional Steel Research, 114: 338-348, 10.1016/j.jcsr.2015.08.017.

Baragetti S., Terranova A., Vimercati M., 2009, Friction behavior evaluation in beryllium–copper threaded connections. International Journal of Mechanical Sciences, 51: 790-796, 10.1016/j.ijmecsci.2009.09.004.

Chen S., Li Q., Zhang Y., An Q., 2011, Finite element analysis of tooth load distribution on P-110S conic threaded connections. International Journal of Pressure Vessels and Piping, 88: 88-93, 10.1016/j.ijpvp.2011.01.004.

Cui F., Li W.J., Wang G.Z., Gu Z.L., Wang Z.S., 2015, Design and study of gas-tight premium threads for tubing and casing. Journal of Petroleum Science and Engineering, 133: 208-217, 10.1016/j.petrol.2015.06.007.

Ferjani M., Averbuch D., Constantinescu A., 2011, A computational approach for the fatigue design of threaded connections. International Journal of Fatigue, 33: 610-623, 10.1016/j.ijfatigue.2010.11.006.

Fransplass H., Langseth M., Hopperstad O.S., 2013, Numerical study of the tensile behaviour of threaded steel fasteners at elevated rates of strain. International Journal of Impact Engineering, 54:19-30, 10.1016/j.ijimpeng.2012.10.009.

Fransplass H., Langseth M., Hopperstad O.S., 2014, Experimental and numerical study of threaded steel fasteners under combined tension and shear at elevated loading rates. International Journal of Impact Engineering, 76: 118-125, 10.1016/j.ijimpeng.2014.08.004.

Le H.R., Stewart F., Williams J.A., 2015, A simplified model of surface burnishing and friction in repeated make-up process of premium tubular connections. Tribol Lett, 59: 35, 10.1007/s11249-015-0562-x.

Lorenzini G., Espinel Lara M.F., Oliveira Rocha L.A., Neves Gomes M.D., Santos E.D.D., André Isoldi L.A., 2015, Constructal design applied to the study of the geometry and submergence of an oscillating water column. International Journal of Heat and Technology, 33(2): 31-38, 10.18280/ijht.330205.

Wu J., Wei Z.Y., Han X.L., 2013, The field inspection and research of related problems about a kind of non-API thread connections. Applied Mechanics and Materials, 300-301: 982-987, 10.4028/www.scientific.net/AMM.300-301.982.

Sønstabøa J.K., Holmstrøm P.H., Morin D., Langseth M., 2015, Macroscopic strength and failure properties of flow-drill screw connections. Journal of Materials Processing Technology, 222: 1-12, 10.1016/j.jmatprotec.2015.02.031.

Yuan G.J., Yao Z.Q., Wang Q.H., Tang Z.T., 2006, Numerical and experimental distribution of temperature and stress fields in API round threaded connection. Engineering Failure Analysis, 13: 1275-1284, 10.1016/j.engfailanal.2005.11.006.

Yeh M.C., Lin Y.L., Huang G.P., 2014, Investigation of the structural performance of glulam beam connections using self-tapping screws. J Wood Sci, 60: 39-48, 10.1007/s10086-013-1376-9.

Zanuy C., Fuente P. de la, Pinilla M., 2012, Bending strength of threaded connections for micropiles. Journal of Constructional Steel Research, 78: 68-78, 10.1016/j.jcsr.2012.06.009.